A wind tunnel study of the impact of upstream obstructions on the performance of vertical axis wind turbines in low-speed wind

Gift Nyamane [1], and T*iyamike* Ngonda [1*]

[1]School of Mechanical, Industrial and Aeronautical Engineering, University of Witwatersrand, Johannesburg, South Africa

Abstract. Vertical-axis wind turbines (VAWTs) are promising for urban renewable energy, but their performance in low-wind, complex-flow conditions is poorly predicted. The quantified effects of obstacle geometry, distance, and height on VAWT start speed and power output remain unknown. This study provides empirical data to close this gap and support optimised siting in marginal wind conditions. A controlled wind-tunnel experiment was performed using a commercial 5-blade drag-based VAWT. Rectangular obstacles (500 × 340 mm) at heights of 600 mm and 750 mm were placed 1, 2 and 3 m upstream. Freestream velocities of 3, 6, 9 and 11 m/s were tested. For each configuration, the electrical power output and rotational speed were measured. The power coefficient (Cp) and start speed were calculated and benchmarked against an unobstructed base case. The study found that the presence of an upstream obstacle significantly enhanced VAWT performance compared to the unobstructed base case. A 43.5% increase in peak power coefficient was achieved with the taller obstacle at 2 m. Furthermore, the turbine start speed was reduced by over 50%, from 2.5 m/s to approximately 1.1 m/s. Performance enhancement was non-monotonic, with optimal distance dependent on obstacle height (1 m for 600 mm; 2 m for 750 mm). This is attributed to a beneficial interaction with the obstacle's wake, in which flow acceleration and turbulent structures simultaneously increase the impulse on the driving blades and reduce the resistance on the returning blades. The study concludes that siting a VAWT behind an upstream bluff body can enhance VAWT performance. These findings are limited to controlled wind tunnel conditions, as the simplified setup does not fully replicate real-world field flows.

1 Introduction

The global energy sector is undergoing a critical transformation, driven by the urgent need to mitigate climate change and ensure energy security. A central pillar of this transition is the ambitious international target to triple renewable energy capacity by 2030 from 2022 levels [1]. This global imperative is reflected in national policies, with South Africa committing to increasing the share of renewable energy in its power generation mix to 40% by 2030 [2]. To operationalise this goal, the South African Renewable Energy Masterplan (SAREM), approved in March 2025, outlines a plan to add 3-5 GW of new renewable capacity annually through 2030 [3].

The predominant technology in utility-scale projects is the Horizontal-Axis Wind Turbine (HAWT) [4]. HAWTs are preferred over VAWTs due to their higher power coefficient [4]. To access consistent, high-velocity laminar wind flows and minimise the impact of ground-level turbulence, HAWTs are mounted on tall towers, often exceeding 100 meters in height, and require substantial spacing (6-15 rotor diameters) to avoid aerodynamic interference (wake effects) between units [4–6].

However, the suitability of HAWTs diminishes drastically in urban and peri-urban environments. Their large size, noise emissions, and requirement for tall, obstructive towers render them impractical for integration into residential or commercial settings. This has spurred interest in distributed generation, in which modular systems, such as rooftop solar PV, are combined with small-scale wind turbines to reduce grid dependence and alleviate pressures, including load shedding.

For urban wind energy, Vertical-axis wind turbines (VAWTs) present a more viable alternative. VAWTs are omnidirectional, meaning they do not need to yaw into the wind, and are inherently better at handling the turbulent and rapidly shifting wind conditions typical of cities [4]. Their operation is generally quieter, and their compact, ground-level or roof-mounted installation is less obtrusive [4, 6]. Notably, studies indicate that VAWT performance can improve in turbulent flow, with one study reporting an 11% increase in the power coefficient when turbulence intensity was increased from 8% to 18% [7].

Despite these advantages, the deployment of rooftop-mounted VAWTs in cities remains challenging. The urban landscape is cluttered with obstacles such as parapets, chimneys, elevator overruns, and adjacent buildings that distort the wind field. These obstacles create complex zones of accelerated flow, increased turbulence, and downstream wakes, all of which

* Corresponding author: tiyamike.ngonda@wits.ac.za

profoundly impact the power output and operational stability of a VAWT [8]. Consequently, the placement of a turbine on a roof, specifically its distance from these obstacles, is a critical design parameter that can affect turbine performance.

Currently, a significant gap exists in the practical guidance available for installers. While it is established that higher turbulence intensity can benefit VAWT performance, this aggregated metric does not provide actionable insight. The specific influence of an obstacle's geometry and, most importantly, the distance between the obstacle and the turbine rotor, as well as the obstacle's height relative to the turbine, remains poorly quantified [9]. Simply knowing that turbulence is high is insufficient; an engineer must know how to position the turbine to exploit this turbulence for optimal power generation and a minimised start speed.

This lack of knowledge presents a tangible risk. Suboptimal turbine placement leads to underperforming installations, failed projects, wasted investment, and ultimately, a loss of confidence in small-scale wind energy as a viable solution for urban South Africa. Therefore, this research is motivated by the critical need to move beyond general turbulence metrics and provide a quantified understanding of how obstacle proximity affects VAWT performance. The stakes are the efficient harnessing of urban wind resources, the economic viability of distributed generation, and ultimately, contributing to South Africa's renewable energy and security goals. This analysis logically leads to the objectives of investigating and optimising turbine placement relative to obstacles.

2 Literature Review

Real-urban terrain flow is characterised by reduced mean wind speed near roof level due to surface roughness and upwind building sheltering, as well as increased turbulence intensity (TI), directional variability, and non-uniform flow [10]. A computational fluid dynamics (CFD) study of an H-Darrieus VAWT on building rooftops under turbulent atmospheric boundary layer inflow found that rooftop positions often experience skewed and elevated turbulence, which can enhance performance relative to uniform inflow, depending on position and height above the roof [11]. Turbulence intensity decreases with increasing height above the ground. This means that, if higher turbulence improves VAWT performance, they can be placed closer to the ground to exploit this effect [12].

In a CFD parametric study [13], A CFD parametric study reported in [13] employed turbulence models to determine the optimal wind turbine position to maximise power capture. It found that mounting a turbine at the edge or just behind the edge of a rooftop resulted in higher air flux due to accelerated flow. However, it also found that recirculation or separation bubbles formed immediately behind the edge [13].

Several key non-dimensional parameters characterise the performance of a VAWT. Once such a parameter is the Tip-Speed Ratio (TSR), which characterises the operational state by linking the rotational speed to the incoming wind speed. Another is the power coefficient (Cp), which quantifies turbine efficiency by measuring the fraction of wind kinetic energy converted into mechanical power.

VAWTs are broadly categorised into drag-based and lift-based designs, each with distinct operational characteristics. Drag-based turbines, such as Savonius turbines, typically achieve peak Cp at low TSR values (0.7–1.2) but suffer from relatively poor efficiency due to negative torque on the returning blade [14]. In contrast, lift-based Darrieus turbines operate optimally at higher TSR (3–5) [15]. This fundamental distinction is crucial for selecting the appropriate turbine technology for a given wind regime.

The wake generated by an upstream bluff body fundamentally alters the inflow conditions for a downstream turbine [16]. This phenomenon was critically investigated in a CFD study that placed a turbine at various longitudinal and lateral positions [16]. The study revealed that lateral placement, relative to the wake centreline, is a performance factor.

Some studies show that where the turbine was positioned laterally offset from the direct wake ($y > 0$), performance increased by at least 10% [16]. This improvement is attributed to the acceleration of deflected wind around the sides of the obstacle. The figure shows velocity contours at different phases of the unsteady vortex shedding cycle, illustrating how high-velocity regions (acceleration zones) form adjacent to the low-velocity wake.

For turbines placed directly behind the bluff body ($y = 0$) within the wake centreline, the closest position (20 m) showed a 12% performance improvement compared to the farthest (60 m) [16]. This suggests that the immediate near-wake region has a higher velocity due to the higher pressure gradient induced by the vortex.

Several experimental studies confirm that turbulence can improve mean performance (power coefficient) for small VAWTs, particularly at low tip-speed ratios (TSR). A study [15] tested an H-Darrieus prototype in two wind tunnels under different turbulence intensities and integral length scales. They found that moving from very low turbulence intensity (0.5%) to moderate turbulence intensity (15%) increased the power coefficient (Cp) by up to 20%, especially at low TSR. Still, this benefit diminished as the Reynolds number exceeded 4×10 ^5 [15].

Literature reveals a significant disconnect between the understanding of urban wind flows and the availability of actionable data for VAWT siting. While existing studies effectively characterise the general urban wind resource and the aerodynamic principles of VAWTs, they fall short of systematically mapping turbine performance as a function of specific obstacle proximity. A research paper on rooftop siting provides valuable insights into flow acceleration and separation at roof edges, but the simulated airflow lacks obstacles [11, 17]. Wind tunnel experiments demonstrate the performance benefits of homogeneous turbulence [15]. However, these approaches do not replicate the fundamental interaction with a discrete, isolated bluff body nor provide a quantitative framework for key metrics such as start speed and power coefficient as

functions of distance and height. Consequently, there is a lack of empirical data that bridges the established principles of bluff-body aerodynamics with practical performance predictions for VAWTs in obstructed, low-wind-speed environments.

3 Research Methods

3.1 Experimental Apparatus and Instrumentation

The experiments were conducted in the blow-down wind tunnel at the University of the Witwatersrand, with a test section of 1.5 m (W) × 1.5 m (H) × 5.89 m (L). The overall setup is shown in Fig. 1. The wind tunnel is limited to a maximum recommended speed of 11 m/s.

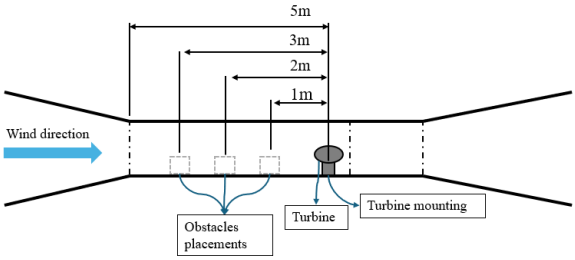

Fig. 1. The overall setup of the wind tunnel test section

A commercial 5-blade VAWT was used, with a rated electrical power of 500 W at 48 V DC. The rotor diameter (D) was 0.9 m, and the rotor height (H) was 0.65 m, resulting in a swept area of 0.46 m². The turbine was connected to a three-phase bridge rectifier (Model: TBR2512DC) to deliver DC power. The electrical load was provided by a rheostat set to a constant resistance of 37 Ω for all tests.

Two rectangular obstacles were fabricated from plywood. Both shared a front face width of 500 mm and a depth of 340 mm, but differed in height: a "short" obstacle at 600 mm and a "tall" obstacle at 750 mm.

The arrangement of the turbine, obstacle, and instrumentation within the wind tunnel test section is illustrated in Fig. 2. The pitot tube for freestream velocity measurement was positioned 4 m upstream of the turbine. The optical tachometer was mounted on a stand, aimed at a reflective marker on the turbine hub. The obstacle was placed on the tunnel centrelines at the specified upstream distances. Note that the obstacles shown by the grey colour in Fig. 2 represent the positions where the obstacle can be placed and not the obstacle itself.

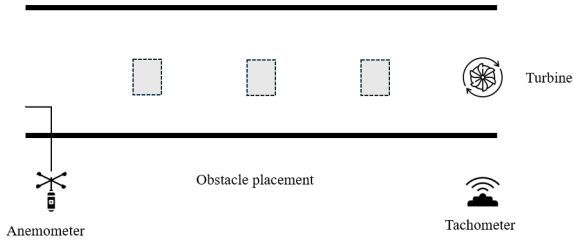

Fig. 2. Schematic illustration of the instrumentation placement and obstacle positions relative to the turbine.

The digital anemometer was used to measure the wind speed. A Fluke 922 Micromanometer has a range of up to 80 m/s, a resolution of 0.001 m/s, and an accuracy of ±2.5 %. The optical tachometer used to measure the turbine's rotational speed has a range of 3 to 99999 r/min and an accuracy of ±(0.05% + 1). The Fluke digital multi-meters for DC voltage in the 6V to 60V range have a resolution of 0.01V, an accuracy of ± (0.5% +2) and for current in the range of 0.001A to 6A, accuracy is ± 2.5%

3.2 Experimental Design and Testing Procedure

A full-factorial test matrix was executed. For each configuration, instruments were validated (see Section 2.2.3) and baseline data were collected with no obstacle present at four freestream velocities: 3, 6, 9, and 11 m/s. For obstructed-flow tests, the selected obstacle (short or tall) was positioned at the prescribed distance (1, 2, or 3 m). The wind tunnel was set to the target velocity and allowed to stabilise for 60 s before steady-state voltage, current, rotational speed (RPM), and freestream velocity were recorded. Each unique condition was repeated three times. Atmospheric conditions (21–23°C, 2–16% RH) were monitored using an Oregon Scientific BAR208HGA to account for air-density variations.

3.3 Data Analysis

The raw data consisted of manually recorded average values for DC voltage (V), DC current (I), rotational speed (RPM), and freestream wind speed (V). These values were immediately transcribed into a structured Microsoft Excel spreadsheet for processing. Calculations were performed for electrical power output, tip-speed ratio, and power coefficient (Cp). The experimental data yielded electrical power. However, Cp required mechanical power, which was calculated based on the assumption that the generator had a constant efficiency.

The turbine supplier provided no information on the turbine's efficiency; thus, an overall system efficiency of η_{eff} = 0.85 was assumed for this study, based on the turbine's specifications and data from other models of the same size. Substituting and rearranging to solve for Cp yields the final equation used:

$$C_p = \frac{P_{elec}}{\eta_{eff} \times \frac{1}{2}\rho A V^3}$$

4 Results

The turbine performance was assessed through two complementary metrics to provide a complete picture of the aerodynamic and practical effects. First, the power coefficient is plotted as a function of the tip speed ratio. This non-dimensional representation is the standard for evaluating the turbine's intrinsic aerodynamic efficiency, thereby isolating its performance from variations in wind speed and rotor size. Second, the electrical power output is plotted as a function of wind speed. This relationship provides a direct measure of the turbine's energy-generation capability across different

operating conditions, which is of paramount importance for practical applications.

Fig. 3 and Fig. 4 detail the performance for the short obstacle

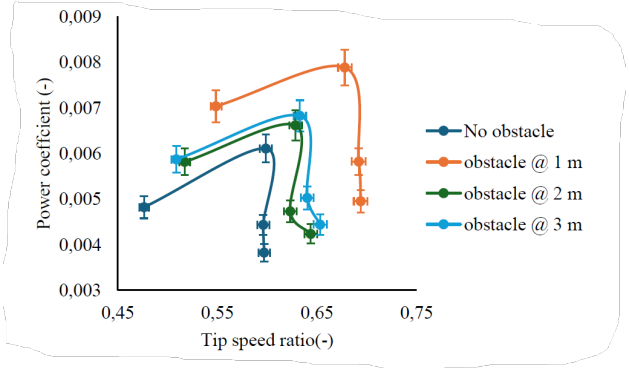

Fig. 3. Power coefficient against the tip speed ratio for the short obstacle

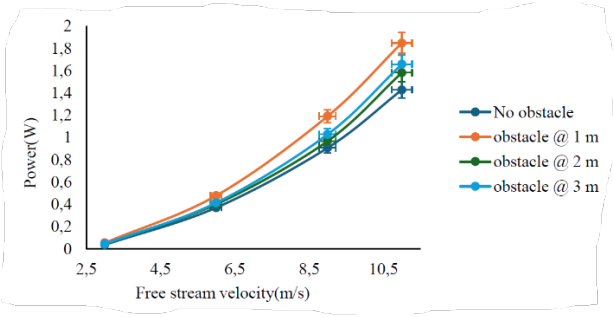

Fig. 4. Electrical power against the free stream velocity for the short obstacle

An identical analysis was performed for the tall obstacle. Fig. 5 presents the power coefficient as a function of tip-speed ratio for the base case and the three distances with the tall (750 mm) obstacle.

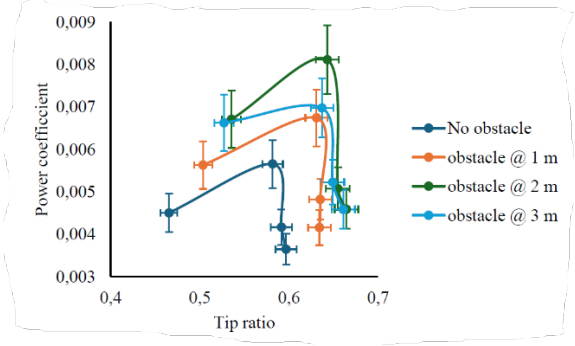

Fig. 5. Power coefficient against the tip speed ratio for the tall obstacle

Fig. 6 presents the curve for power generation for the tall obstacle configurations

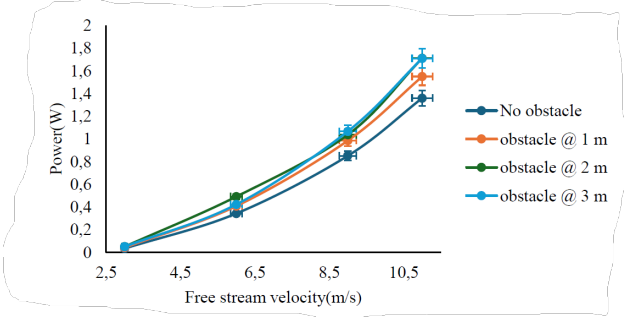

Fig. 6. Electrical power against the free stream velocity for the tall obstacle

Fig. 7 shows the measured start speeds for all test configurations, providing a clear comparison of the turbine's operational threshold under each condition.

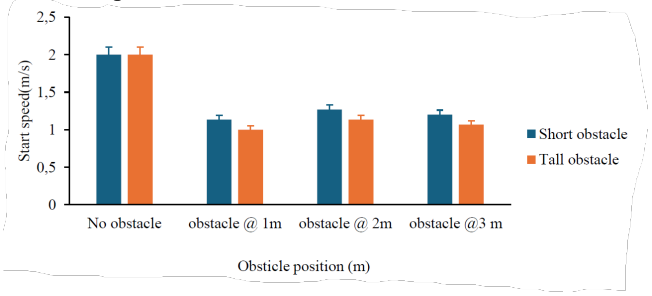

Fig. 7. Start speed against the obstacle position for the short obstacle and tall obstacle

5 Discussion

The experiments show that a VAWT performs better when placed behind an upstream obstacle than in unobstructed flow for the tested configurations, though this is not a universal result. The unobstructed case serves as the reference.

For the short obstacle baseline (Fig. 3), the Cp peaks at 0.0061 at a tip-speed ratio of ~0.60 and at 76.23 rpm. For the tall obstacle baseline (Fig. 5), the peak CP is 0.0057 at a tip-speed ratio of ~0.58 and at 74.07 rpm. Although low in absolute terms, these values provide a consistent baseline. The Cp curves peak and then decline, as is typical of drag-based VAWTs, reflecting the trade-off between increasing torque and increasing drag on the returning blade. The base-case electrical power curves (Fig. 4 and 6) follow the expected cubic dependence on wind speed ($P \propto V^3$). The start speed is 2.5 m/s for both baselines (Fig. 7).

In contrast to HAWT siting guidelines that favour unobstructed flow, the data show that an upstream bluff body can significantly enhance VAWT performance. The effect is substantial and repeatable, with higher peak Cp and much lower start speed.

With the short obstacle at 1 m upstream, the peak CP increases from 0.00611 to 0.00789 (29.1% gain), and the Cp curve lies above the baseline across the operating range. Electrical power also increases: at 6 m/s from 0.370 W to 0.477 W (29%); at 11 m/s from 1.426 W to 1.847 W (29.5%) (Fig. 4). Obstacles at 2 m and 3 m still improve performance. Still, less than at 1 m, indicating a non-monotonic distance effect.

The tall obstacle yields an even greater benefit, with the optimum at 2 m upstream. The peak Cp increases from 0.0057 to 0.0081 (43.5%; Fig. 5). At 6 m/s, electrical power increases from 0.342 W to 0.491 W (43.6%, Fig. 6). The consistent scaling of CP and power confirms a genuine aerodynamic effect rather than measurement error.

The most important practical result is the substantial reduction in start speed (Fig. 7). The baseline 2.5 m/s is reduced to ~1.1 m/s for the short obstacle at 1 m and 2 m, and to ~1.2 m/s for the tall obstacle at 1 m and 2 m. This substantially widens the operating envelope, enabling power generation in low-wind urban environments and increasing annual energy yield.

Performance does not vary linearly with obstacle distance but shows clear optima. For the 600 mm obstacle: 1 m > 2 m > 3 m > No Obstacle. For the 750 mm obstacle: 2 m > 3 m ≈ 1 m > No Obstacle. This non-monotonic behaviour reflects complex wake dynamics: beneficial effects dominate at the optimal distance, while detrimental effects increase when the obstacle is too close or too far. The shift in optimal distance with obstacle height indicates that placement is governed by wake geometry, which scales with obstacle size.

The shell-like VAWT blades generate torque from the force difference between the concave (driving) and convex (returning) sides. Enhancement must therefore increase impulse on the driving side, reduce resistance on the returning side, or both. The hypothesis is that the upstream obstacle alters the flow field to achieve this via wake turbulence and flow constriction, which augment momentum, energise blade boundary layers, and suppress negative-torque vortices.

These findings provide experimental support for prior computational and theoretical work on flow manipulation in VAWT arrays, where downstream turbines can sometimes benefit from upstream wakes. Naseem et al. [16] reported 12–24% performance gains for VAWTs placed behind a bluff building and ~13% velocity increase for specific configurations. Other studies show that increased turbulence intensity can raise VAWT Cp [15]. While direct studies of this exact configuration are limited, related work is consistent with the observed results.

Overall, enhancements up to 43.5% in peak CP are achievable, directly challenging siting guidelines derived from HAWTs. Optimal performance occurs at obstacle-height-dependent distances (1 m for a 600 mm obstacle; 2 m for a 750 mm obstacle). The critical practical outcome is the reduction of start speed from 2.5 m/s to ~1.1 m/s, enabling viable deployment in low-wind urban sites. The primary mechanism is attributed to the beneficial interaction between the obstacle wake and the turbine, and the study successfully meets its core research objective.

5.1 Limitations of the Study

This section examines how methodological limitations may influence the results. Although relative performance trends across configurations are clear, several experimental factors must be acknowledged to contextualise the absolute values and interpret them accurately within wind energy research. These limitations are typical of small-scale wind tunnel testing and do not invalidate the core findings; instead, they define the realistic scope of applicability.

The power coefficients in this study, consistently below 0.01, are substantially lower than those reported in previous work. This results from fundamental scaling laws and the chosen turbine design. First, the generator is effectively rated for much lower power than specified by the manufacturer; technician testing confirmed that it produces an order-of-magnitude lower power output than it should. Second, the turbine's drag-based operating principle is inherently less efficient than lift-based aerodynamics, whose theoretical maximum Cp is much higher. Consequently, the absolute Cp values here should be regarded as indicative, not as precise measures of the rotor's pure aerodynamic efficiency.

A primary concern is wind-tunnel blockage, in which the model constrains the flow, accelerating it around the body and artificially increasing the effective freestream velocity. Recommended tunnel blockage is 5%–10%, while the wind turbine's swept area is 26%, causing an overestimation of the actual power coefficient. Additional systematic errors may have arisen from minor drift in instrumentation calibration over the long test campaign or from thermal effects that altered the generator's electrical characteristics under load. Still, the consistency of relative trends suggests these were secondary.

6 Conclusion

This experimental investigation demonstrates that, under controlled wind tunnel conditions, upstream obstacles can significantly enhance the performance of a drag-based VAWT. The measured increases in power coefficient (up to 43.5%) and reductions in start speed (up to 50%) are substantial. The effect is non-monotonic and depends on both obstacle height and distance, suggesting that the scaling laws of bluff-body wake interaction govern performance. The optimal siting distance was identified as the position where the wake provides favourable pressure differentials and turbulent energy to the turbine blades.

However, it must be emphasised that these results, while conclusive within the context of this study, require validation in real-world conditions. The precise performance gains and the underlying fluid mechanisms, while strongly indicated, cannot be definitively confirmed without field testing. The observed benefits may be influenced by wind-tunnel constriction and simplified inflow turbulence. Therefore, within the scope of this laboratory study, the key recommendation for turbine placement is to position it at a specific, obstacle-height-dependent distance (e.g., 1 m for a 600 mm obstacle; 2 m for a 750 mm obstacle) to exploit the beneficial wake interaction.

References

1. IEA, COP28 Tripling Renewable Capacity Pledge, Paris, 2024. https://www.iea.org/reports/cop28-tripling-renewable-capacity-pledge
2. K. Ukoba, T.-C. Jen, and A. A. Yusuf, Transformation of South Africa's energy landscape: Policy implications, opportunities, and technological innovations in the Fourth Industrial Revolution, Energy Strategy Rev., **59**, 101752, (2025), doi: 10.1016/j.esr.2025.101752.
3. [T. Ivanova, South Africa approves plan to boost renewable energy by up to 5 GW annually, Renewables Now. https://renewablesnow.com/news/south-africa-approves-plan-to-add-up-to-5-gw-of-renewables-annually-1273583/

4. H. Eftekhari, A. Sh. M. Al-Obaidi, and S. Eftekhari, Aerodynamic Performance of Vertical and Horizontal Axis Wind Turbines: A Comparison Review, Indones. J. Sci. Technol., **7**(1), 65–88, (2021), doi: 10.17509/ijost.v7i1.43161.
5. M. Kinzel, Q. Mulligan, and J. O. Dabiri, Energy exchange in an array of vertical-axis wind turbines, J. Turbul., **13**, N38, (2012), doi: 10.1080/14685248.2012.712698.
6. M. A. Al-Rawajfeh and M. R. Gomaa, Comparison between horizontal and vertical axis wind turbine, Int. J. Appl. Power Eng., **12**(1), 13–23, (2013).
7. E. Möllerström, S. Eriksson, A. Goude, F. Ottermo, and J. Hylander, Turbulence influence on optimum tip speed ratio for a 200 kW vertical axis wind turbine, J. Phys. Conf. Ser., **753**, 032048, (2016), doi: 10.1088/1742-6596/753/3/032048.
8. K. C. S. Kwok and G. Hu, Wind energy system for buildings in an urban environment, J. Wind Eng. Ind. Aerodyn., **234**, 105349, (2023), doi: 10.1016/j.jweia.2023.105349.
9. C. Phillips et al., Evaluation of obstacle modelling approaches for resource assessment and small wind turbine siting: case study in the northern Netherlands, Wind Energy Sci., **7**(3), 1153–1169, (2022), doi: 10.5194/wes-7-1153-2022.
10. S. Emeis, K. Baumann-Stanzer, M. Piringer, M. Kallistratova, R. Kouznetsov, and V. Yushkov, Wind and turbulence in the urban boundary layer analysis from acoustic remote sensing data and fit to analytical relations, Meteorol. Z., **16**(4), 393–406, (2007), doi: 10.1127/0941-2948/2007/0217.
11. P. Zamre and T. Lutz, Computational-fluid-dynamics analysis of a Darrieus vertical-axis wind turbine installation on the rooftop of buildings under turbulent-inflow conditions, Wind Energy Sci., **7**(4), 1661–1677, (2022), doi: 10.5194/wes-7-1661-2022.
12. C. Paula, C. José, M. Leorlen, G. Daniel, C. Alexandre, and S. Teresa, “Wind Resource Assessment in Building Environment: Benchmarking of Numerical Approaches and Validation with Wind Tunnel Data,” Wind, vol. 2, no. 4, pp. 659–690, Oct. 2022, doi: 10.3390/wind2040035.
13. S. M. Ishfaq and H. N. Chaudhry, Numerical investigation of the optimum wind turbine sitting for domestic flat roofs, Sustain. Build., **3**, 2, (2018), doi: 10.1051/sbuild/2018001.
14. A. G. Chitura, P. Mukumba, and N. Lethole, Enhancing the Performance of Savonius Wind Turbines: A Review of Advances Using Multiple Parameters, Energies, **17**(15), 3708, (2024), doi: 10.3390/en17153708.
15. A. Carbó Molina, T. De Troyer, T. Massai, A. Vergaerde, M. C. Runacres, and G. Bartoli, Effect of turbulence on the performance of VAWTs: An experimental study in two different wind tunnels, J. Wind Eng. Ind. Aerodyn., **193**, 103969, (2019), doi: 10.1016/j.jweia.2019.103969.
16. A. Naseem et al., Effect of vortices on power output of vertical axis wind turbine (VAWT), Sustain. Energy Technol. Assess., **37**, 100586, (2020), doi: 10.1016/j.seta.2019.100586.
17. Q. Wang, J. Wang, Y. Hou, R. Yuan, K. Luo, and J. Fan, Micrositing of roof mounting wind turbine in urban environment: CFD simulations and lidar measurements, Renew. Energy, **115**, 1118–1133, (2018), doi: 10.1016/j.renene.2017.09.045.